Vol 17 No 12, December 2008
1674-1056/2008/17(12)/4673-04

Chinese Physics B

© 2008 Chin. Phys. Soc.
and IOP Publishing Ltd

Off-axis dose distribution for rectangle proton beam*

Gou Cheng-Jun(勾成俊)†, Luo Zheng-Ming(罗正明), Huang Chu-Ye(黄初叶),
Feng Xiao-Ning(冯晓宁), and Wu Zhang-Wen(吴章文)‡

Key Laboratory of Radiation Physics and Technology (Sichuan University), Ministry of Education and Institute of Nuclear Science and Technology, Sichuan University, Chengdu 610064, *China*

(Received 1 May 2008; revised manuscript received 1 June 2008)

This paper modifies an analytical algorithm originally developed for electron dose calculations to evaluate the off-axis dose distribution of rectangle proton beam. This spatial distribution could be described by Fermi–Eyges theory since a proton undergoes small-angle scattering when it passes through medium. Predictions of the algorithm for relative off-axis dose distribution by a 6 cm * 6 cm initial monoenergetic proton beam are compared with the results from the published Monte Carlo simulations. The excellent level of agreement between the results of these two methods of dose calculation ($< 2\%$) demonstrates that the off-axis dose distribution from rectangle proton beam may be computed with high accuracy using this algorithm. The results also prompts the necessity to consider the off-axis distribution when the proton is applied to clinical radiotherapy since the penumbra is significant at the distal of its range (about 0.6 cm at the Bragg-peak depth).

Keywords: proton, radiotherapy, Fermi–Eyges
PACC: 8770H, 8760M

1. Introduction

Significance of proton beam radiotherapy is increasing recently.[1−6] For therapeutic proton beams, a proton will undergo inelastic and elastic Coulomb interactions when it passes through the water phantom or tissue. During inelastic Coulomb interactions in materials, protons are slowed down when they lose their kinetic energy, mainly through ionization of the medium. If we assumed that the secondary electrons produced by the inelastic interaction deposited their energy locally and neglected the energy-loss fluctuations, the protons would be expected to lose their energy continuously along their tracks at a rate given by the stopping power. Since the proton's stopping power is approximately proportional to the inverse square of the proton velocity, the energy acquired by the medium from the incident proton forms a localized Bragg peak with a sharp distal falloff at the end of the travelling path of the proton, where the remaining energy approaches zero.

For a proton beam, its energy is deposited mainly near the depth where the Bragg peak locates. Beyond the Bragg-peak depth, the dose is decreased sharply and down to zero quickly. The Bragg-peak depth is as a function of the initial energy of the incident proton. This character provides proton beam a wider prospect in the field of radiotherapy than that of photon beam and electron beam. For example, we can deliver the proton's energy to the tumour as much as possible, at the same time, little or none energy to the organs at risk (OAR) or healthy tissues by carefully choosing incident energy of proton beams to ensure that their Bragg peak is at the tumour depth. However, for photon beam, a comparative fraction of energy is always delivered to the deeper position, where OARs or healthy tissues exist. And for electron beam, although the energy deposition is sharply decreased at its range distal, its range is always short and has high surface dose.

For another hand, when a proton penetrates a medium, it undergoes not only inelastic interaction which loses its energy with the media, but also Coulomb elastic interaction, which causes the proton to deviate from its initial incident direction. This action will result in the proton's expanding along the off-axis direction, which is perpendicular to the incident direction (z direction), and affects the critical organs located adjacent to the proton beam edge. Moreover, the expanding effect becomes significant at the

*Project supported by the State Key Program of National Natural Science of China (Grant No 10335050).
†E-mail: ChengJ.Gou@263.net
‡E-mail: wuzhangwen@gmail.com

depth near the end of proton's track. In order to accurately evaluate the dose effect on the healthy tissues and OARs near the edge of the proton beam, we should comprehensively understand the off-axis dose distribution of a rectangle proton beam.

This paper modifies an analytical algorithm originally developed for electron dose calculations[7−10] to calculate off-axis dose of a rectangle proton beam. When we calculate the off-axis dose distribution of an electron beam, a Gaussian spatial distribution is introduced by considering the electron's elastic scattering with medium. This work uses the same method but uses the Rutherford scattering formula instead when we calculate the scattering term. In the next section, we will introduce the algorithm. And in the last section, we will illustrate and discuss some results of the method.

2. Algorithm

As a modification of a dose algorithm originally developed for therapeutic high energy electron beams, the algorithm described in this section may be used to compute off-axis dose distribution in homogeneous media irradiated by a proton beam with rectangular or square shape. Assuming that there is a mono-energetic and mono-directional infinite narrow proton beam, i.e. a pencil proton beam, with energy E_0 normally incident upon the surface of an infinitely uniform medium, we define the origin of the coordinate system as the point upon which the proton is incident and the positive z direction as the same direction of the incident proton. The x-, y- and z-axis are chosen to be mutually perpendicular and form a Cartesian coordinate system. Then we can get the spatial distribution of proton beam as

$$H(x,y,z)=\frac{1}{4\pi A_2(z)}\exp\left(-\frac{x^2+y^2}{4A_2(z)}\right). \tag{1}$$

This formula can be obtained as the similar process as electron's HPBM algorithm[7−10] with

$$A_2(z)=\frac{1}{4}\int_0^z T(E_a(\eta))(z-\eta)^2\,\mathrm{d}\eta, \tag{2}$$

$$T(E)=\sum_i 2\pi N_i\int_0^\pi \sin^2\theta[\sigma_i(E,\theta)+Z_i\sigma_e(E,\theta)]\sin\theta\mathrm{d}\theta, \tag{3}$$

where $T(E)$ is the scattering power, $E_a(z)$ is the average energy of protons at depth z, N_i is the number of the i-th kind of atom whose atomic number is Z_i in unit volume of the target, σ_i is the elastic scattering differential cross section caused by protons colliding with the i-th kind of target atoms, σ_e is the elastic scattering differential cross section between protons and target electrons.

Using the revised Rutherford formula, we can get the differential scattering cross section of protons for the i-th kind of atom in medium, and then we have the scattering power as follows:[11]

$$T(E)=2\pi r_0^2\left(\frac{m_e}{m_p}\right)^2\left[\frac{\tau+1}{\tau(\tau+2)}\right]^2\sum_i N_iZ_i(Z_i+1)\left[\left(\chi_a^2+2\right)\ln\left(1+\frac{4}{\chi_a^2}\right)-4\right], \tag{4}$$

$$\chi_a^2=\hbar^2Z_i^{2/3}\frac{1.13+3.76(\alpha Z_i)^2}{(0.8853a_0m_pc)^2}\frac{(\tau+1)^2}{\tau(\tau+2)}, \tag{5}$$

where, r_0 is the classical electron radius, m_e is the rest mass of an electron, m_p is the mass of a proton, τ is the proton energy in unit of its rest energy, $\hbar$ is the Planck constant, a_0 is Bohr radius, α is the fine structure constant and c is the velocity of light.

For a rectangle proton beam with $2a*2b$ size, its spatial dose distribution is the integral of the dose distribution of a pencil of proton beam over x- from -a to a and y- from -b to b respectively, and can be written as:

$$\begin{aligned}D_P(x,y,z)&=\int_{-a}^{a}\mathrm{d}x'\int_{-b}^{b}\mathrm{d}y'D_H(x-x',y-y',z)\\&=\frac{D(z)}{4}\left[\mathrm{erf}\left(\frac{a+x}{\sqrt{A_2(z)}}\right)+\mathrm{erf}\left(\frac{a-x}{\sqrt{A_2(z)}}\right)\right]\left[\mathrm{erf}\left(\frac{b+y}{\sqrt{A_2(z)}}\right)+\mathrm{erf}\left(\frac{b-y}{\sqrt{A_2(z)}}\right)\right],\end{aligned} \tag{6}$$

where, $D(z)$ is depth dose of an infinite width proton beam, which can be gotten by the method introduced by Wang *et al*,[6] and erf(x) is error function.

3. Comparison of results

A comparison of results of the scattering power $T(E)$ for proton in aluminium between our calculation (solids) and data from Janni[12] (squares) is illustrated in Fig.1. This comparison shows that the two results have a good agreement when the proton energy varies from 1 keV to 10 GeV. At the same time, the scattering power for proton in water (dots) is presented in the same figure.

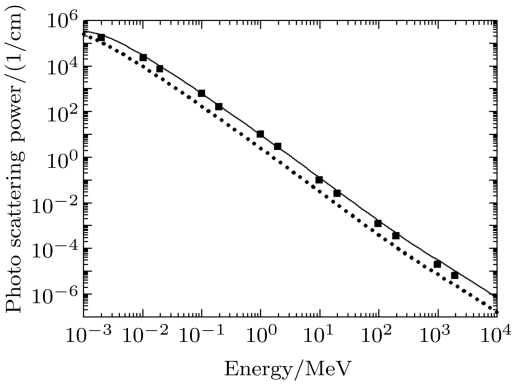


Fig.1. Scattering power of protons with energy from 1 keV to 10 GeV in aluminium and water. Square: the results in aluminium given by Janni. Solid and dots: our calculated results for proton in aluminium and water respectively.

In Eq.(1) $A_2(z)$ is a function of depth. Figure 2 presents the $A_2(z)$ for a 160 MeV proton beam, which is normally incident on water phantom. It shows that the A_2 becomes larger and larger when the depth increases. This means that the proton deflected from its initial direction is more significant as the depth increases because of the elastic interaction with the medium.

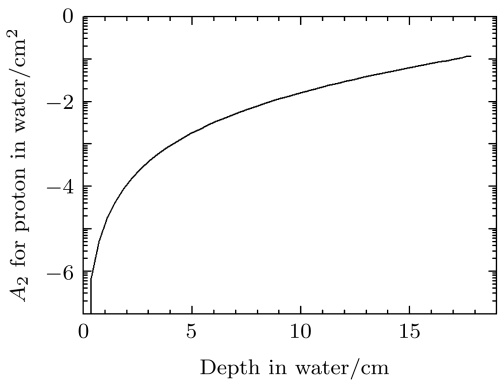


Fig.2. The $A_2(z)$ for a 160 MeV proton beam normally incident on water phantom.

Comparisons between our calculative results (solid lines) and MCNPX results (dots), by Sandison *et al*[3] are illustrated in Fig.3. There only exists little discrepancy at the outer beam (about 3 cm off-axis distance). The maximum disagreement is less than 2%.

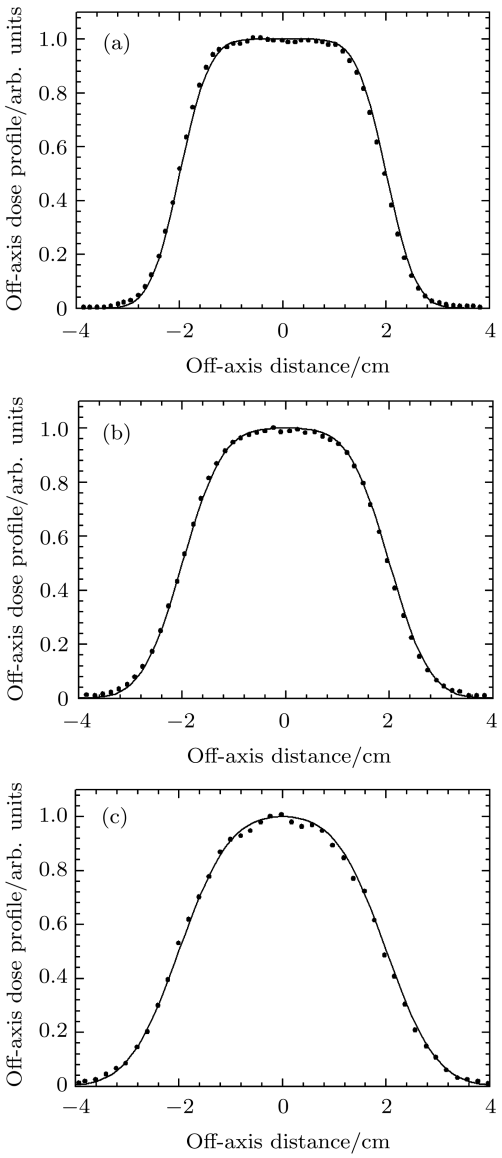


Fig.3. Off-axis dose profiles along the x-axis at the Bragg-peak depth for various proton beams in water. The data show results from our calculations (solid lines) and MCNPX (dots) calculations by Sandison *et al*, which are normalized to the maximum dose at the Bragg peak position. (a) Average beam energy $E = 158.5$ MeV, Gaussian energy spread $S_E/E = 0.95\%$. (b) Average beam energy $E = 188.4$ MeV, Gaussian energy spread $S_E/E = 0.5\%$. (c) Average beam energy $E = 214.5$ MeV, Gaussian energy spread $S_E/E = 0.4\%$.

Our method is also performed by using a simple uniform water phantom with a $6*6\,\mathrm{cm}^2$ parallel monoenergetic proton beam which is incident normally on the phantom's surface. The initial energy of the proton beam is 160 MeV with range, denoted by R, of $17.65\,\mathrm{g/cm}^2$. Figure 4 shows the off-axis profiles at different depth of $0.5R$, $0.9R$ and Bragg-peak position. The radiation widths of 10%, 20%, 50%, 80% and 90% of centre axis dose at every depth are listed in Table 1. It shows that the width is almost as 6 cm of 50% dose at all depth, this is reasonable since the rectangle beam is parallel. The irradiated region for lower dose is expanded. At the depth of $0.5R$, the radiation width of 10% dose is 6.37 cm with expanding about 6%. At the depth of $0.9R$ and Bragg peak, the expanding is up to 16% and 20% respectively. It is obvious that the critical organs adjacent to the beam edge would be affected significantly at the distal of the proton's range.

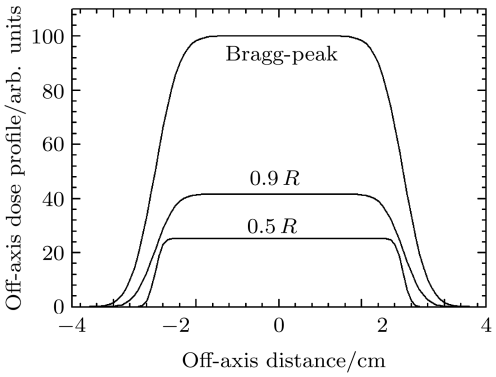


Fig.4. Off-axis dose profiles along the x- axis at different depth for a parallel monoenergetic square proton beam with 160 MeV energy and 6 cm*6 cm field. The calculative results are normalized to the maximum dose at the Bragg peak.

Table 1. The radiation width at different depth for a parallel, monoenergetic rectangle proton beam (with energy being 160 MeV and field being 6 cm∗6 cm), whose range (R) is $17.65\,\mathrm{g/cm}^2$.

Depth	/% 10	20	50	80	90
$0.5R$	6.37	6.23	5.99	5.77	5.61
$0.9R$	6.94	6.67	5.99	5.31	6.96
Bragg peak	7.21	6.78	5.99	5.20	4.80

4. Discussion

In this paper, an analytical algorithm originally developed for electron dose calculations has been modified to evaluate the off-axis dose distribution of a rectangle proton beam. Comparison of results shows that this method is effective. And the calculative results show that it is necessary to take the proton's elastic scattering into account in clinical radiotherapy. In our next work, we shall extend this method to deal with a heterogeneous medium other than homogeneous medium.

References

[1] Thomas B 1997 *Med. Phys.* **24** 2024

[2] George A S, Lee C C, Lu X Y and Lech S P 1997 *Med. Phys.* **24** 841

[3] George C, Jerimy C P, Martin B and Alfred R S 2005 *Med. Phys.* **32** 3511

[4] Asa K C, Pedro A and Anders B 1997 *Phys. Med. Biol.* **42** 1033

[5] Yang D L, Wu Z W, Jiang S B and Luo Z M 2004 *Chin. Phys. Lett.* **21** 2547

[6] Wang Y G and Luo Z M 2000 *Acta Phys. Sin.* **49** 1639 (in Chinese)

[7] Gou C J, Wu Z W, Luo Z M and David J 2003 *Med. Phys.* **30** 415

[8] Luo Z M, David J and Suzan W 1998 *Med. Phys.* **25** 1954

[9] Gou C J, Zeng G and Luo Z M 2003 *Acta Phys. Slov.* **53** 259

[10] Gou C J, Yang D L, Zeng G and Luo Z M 2002 *Acta Phys. Sin.* **51** 2649 (in Chinese)

[11] Moliere G 1947 *Z. Naturforsch.* A **2** 133
Moliere G 1948 *Z. Naturforsch.* A **3** 78

[12] Janni J F 1982 *Atomic Data Nucl. Data Tables* **27** 147